Quasiparticle Scattering in a Superconductor near a Nematic Critical Point: Resonance Mode and Multiple Attractive Channels

Dimitri Pimenov,* Alex Kamenev, and Andrey V. Chubukov
William I. Fine Theoretical Physics Institute, University of Minnesota, Minneapolis, Minnesota 55455, USA

(Received 29 June 2021; accepted 1 December 2021; published 6 January 2022)

We analyze the scattering rate for 2D fermions interacting via soft nematic fluctuations. The ground state is an s-wave superconductor, but other pairing channels are almost equally attractive. This strongly alters the scattering rate: At energies beyond the pairing gap Δ, it is renormalized by contributions from all pairing channels. At energies of order Δ, it is determined by the competition between scattering into a gapped continuum and dispersing nematic resonance. The outcome is a "peak-peak-dip-hump" spectrum, similar, but not identical, to the "peak-dip-hump" structure in the cuprates.

DOI: 10.1103/PhysRevLett.128.017001

Introduction.—The spin resonance mode, observed in a number of quasi-2D cuprate superconductors at momentum (π,π), has attracted much attention in the studies of high-temperature superconductivity [1–3]. The resonance mode mediates a 4-fermion interaction and accounts for the "peak-dip-hump" structure of the fermionic spectral function observed in ARPES measurements [4–9]. In an itinerant approach, the resonance can be viewed as a spin exciton, whose emergence below the threshold for the continuum is associated with the d-wave symmetry of a gap function (see, e.g., Refs. [10,11] and references therein).

In this Letter, we argue that a similar phenomenon takes place in a 2D s-wave superconductor near a quantum critical point (QCP) towards a charge nematic order. We demonstrate that the nematic propagator possesses a charge exciton at a frequency $\Omega_{\rm res}(\boldsymbol{q})$, which near an instability is far below the threshold for the continuum at twice the gap value, 2Δ. A nematic resonance at $\boldsymbol{q}=0$ has been observed in the B_{1g} Raman spectra of several iron-based superconductors [12–16]; here we show that $\Omega_{\rm res}(\boldsymbol{q})$ and the spectral weight of the resonance are strongly $\boldsymbol{q}$ dependent, which is tied to the $(\omega/|\boldsymbol{q}|)$ form of the Landau damping of a nematic propagator in the normal state. We analyze how the dispersing charge exciton affects the fermionic spectral function at energies above the threshold at $\Delta+\Omega_{\rm res}(\boldsymbol{q}=0)$. We find that the spectral function is highly nonmonotonic due to strong momentum dependence of $\Omega_{\rm res}(\boldsymbol{q})$. In contrast, a spin resonance in a d-wave superconductor does not lead to such behavior as there relevant momenta $\boldsymbol{q}$ are close to (π,π).

We further analyze the form of the spectral function at energies above 3Δ, when the key contribution comes from the continuum in the nematic propagator. Here, we reveal additional physics of a nematic QCP. Namely, for an isotropic fermionic dispersion, the interaction, mediated by nematic fluctuations, yields an attraction in all pairing channels. The s-wave coupling is the largest one, but only by a small number, proportional to the distance to a nematic transition [17,18]. The continuum part of the order parameter propagator has contributions from all pairing channels, and the fermionic self-energy and the spectral function due to interaction with the continuum are very different from the ones expected for a pure s-wave superconductor. We single out the s-wave contribution and show that it only accounts for a small portion of the full self-energy. We show that at even larger frequencies the self-energy due to interaction with a continuum gradually approaches the normal state result, obtained by summing up a series of logarithmical contributions from backscattering.

Superconductivity at the onset of a nematic order occurs in the much studied $FeSe_{1-x}S_x$—nematic order at $x\leq 20\%$ (see, e.g., Ref. [19] and references within). Our results for the spectral function can be verified in ARPES measurements around the critical doping.

Model and normal state results.—We consider a system of 2D itinerant spin-1/2 fermions on a square lattice near a QCP towards a d-wave nematic order that breaks the fourfold rotation symmetry. We assume that the interaction between fermions is mediated by soft fluctuations of the nematic order parameter. An appropriate Euclidean action is [20]

$$\mathcal{S}=\sum_{\sigma}\int_{k}\bar{\psi}_{\sigma}(k)(-i\omega_{m}+\xi_{\boldsymbol{k}})\psi_{\sigma}(k)+\frac{g}{V}\sum_{\sigma,\sigma'}\int_{k,p,q}D(q)\times f(\boldsymbol{k})f(\boldsymbol{p})\bar{\psi}_{\sigma}\left(k+\frac{q}{2}\right)\bar{\psi}_{\sigma'}\left(p-\frac{q}{2}\right)\times\psi_{\sigma'}\left(p+\frac{q}{2}\right)\psi_{\sigma}\left(k-\frac{q}{2}\right).\tag{1}$$

Here, $f(\boldsymbol{k})$ is a form factor with d_{xy} or $d_{x^2-y^2}$ symmetry, g is the effective fermion-boson coupling, and

$$D(q) = -\frac{1}{M^2 + |\boldsymbol{q}|^2 + g\Pi(q)}, \tag{2}$$

where M measures the small deviation from the QCP and $\Pi(q)$ is the dynamical polarization, induced by the fermions, which has to be computed within the effective action of Eq. (1). $D(q)$ should be seen as an effective interaction which includes both renormalizations from low-energy [via $\Pi(q)$] and high-energy fermions, compare Ref. [21]. Equation (1) can be derived from, e.g., a multiorbital tight-binding model, rotated to the band basis, similar to Ref. [22]. The same effective action emerges in an isotropic system near a d-wave Pomeranchuk instability. In the latter case, $f_{\boldsymbol{q}}(\boldsymbol{k}) = \cos(2\theta_{\boldsymbol{kq}})$ $[\theta_{\boldsymbol{kq}} = \measuredangle(\boldsymbol{k}, \boldsymbol{q})]$, invariant under simultaneous rotation of $\boldsymbol{k}$, $\boldsymbol{q}$. The key physics is the same in both cases, and to simplify the presentation, we focus on the isotropic case and later discuss the changes introduced by the lattice.

The effective interaction $gD(q)$ leads to much studied non-Fermi liquid behavior at $M \to 0$ (Refs. [20,23–25]) and also gives rise to an attraction in different pairing channels. The model has two dimensionless parameters

$$\epsilon = \frac{M}{k_F} \quad \text{and} \quad \lambda = \frac{g}{4\pi v_F M}. \tag{3}$$

The first one is a measure of the distance to a QCP and the second parametrizes the coupling strength. In the immediate vicinity of a QCP, λ is large and the system necessary falls into a strong coupling regime. In our study we focus on the system behavior at small ϵ, but in a theoretically manageable Fermi liquid (FL) regime $\lambda \ll 1$. To this end, we consider the double limit $\epsilon \ll 1$ and $g \ll E_F$, taken such that $\epsilon \ll \lambda \ll 1$ (which implies $\epsilon \gg g/E_F$, setting a lower bound on M [26]). In this situation, the pairing instability develops at typical energies of order $e^{-1/\lambda}$, which remain well inside the FL regime. For example, in $FeSe_{1-x}S_x$ the appropriate parameter window could be reached by increasing the sulfur doping x or pressure beyond the quantum-critical value, where $\epsilon = 0$, $\lambda > 1$, which increases M and therefore increases (decreases) ϵ (λ). Our primary interest is the retarded fermionic scattering rate $\mathrm{Im}[\Sigma^R(k)]$ $[[G^R(k)]^{-1} = [G_0^R(k)]^{-1} + \Sigma^R(k), k = (\omega, \boldsymbol{k})]$. We set $\boldsymbol{k} = \boldsymbol{k}_F$, in which case $\Sigma^R(k) \equiv \Sigma^R(\omega)$. We begin by listing the normal state results, which will serve as benchmarks for our calculations of $\mathrm{Im}[\Sigma^R(\omega)]$ in a superconductor. In the normal state, the polarization bubble at small frequencies has a Landau-damping form, $\Pi(q) = 2\rho|\omega_m|/(v_F q)$, where $\rho = k_F/(2\pi v_F)$ is the density of states (DOS) per spin. At the one-loop level the scattering rate has the familiar 2D FL form [27,28]

$$\mathrm{Im}[\Sigma^{R,(1)}(\omega)] = \frac{2\lambda}{\pi}\frac{\omega^2}{\omega_{\mathrm{FL}}}\ln\left(\frac{\omega_{\mathrm{FL}}}{|\omega|}\right). \tag{4}$$

The logarithm comes from forward-scattering and backscattering processes, which play a special role in two dimensions (Ref. [28]), and $\omega_{\mathrm{FL}} = v_F M^3/g\rho$ sets the upper edge of the FL behavior; our analysis is valid at $\omega < \omega_{\mathrm{FL}}$. At higher loop orders higher powers of the logarithm from multiple backscattering processes appear. They collectively change the scattering rate to [29]

$$\mathrm{Im}[\Sigma^R(\omega)] = \frac{\omega^2}{\pi\omega_{\mathrm{FL}}} \times \left[\frac{\epsilon^2}{4(1-\ell)} - \frac{(1-\ell)\ln^2(1-\ell)}{\ell} + 2\mathrm{Li}_2(\ell)\right], \tag{5}$$

where $\ell = \lambda\ln(\omega_{\mathrm{FL}}/|\omega|)$ and $\mathrm{Li}_2(\ell)$ is a polylogarithm. We plot $\mathrm{Im}[\Sigma^R(\omega)]$ in Fig. 1. This expression becomes singular at $\ell = 1$, i.e., at $\omega \simeq \omega_{\mathrm{FL}} e^{-1/\lambda}$ and is invalid at smaller ω. The reason for this becomes clear once we note that the series of logarithms that transform Eq. (4) into Eq. (5) come from backscattering processes, which involve vanishingly small total momentum and are therefore the same as Cooper processes. The increase of $\mathrm{Im}[\Sigma^R(\omega)]/\omega^2$ with decreasing ω implies that the pairing interaction is attractive, hence the ground state must be a superconductor, and at $\ell = 1$, ω is of order of an expected pairing gap $\Delta = \omega_{\mathrm{FL}} e^{-1/\lambda}$. This clearly shows that the apparent singularity in Eq. (5) is the consequence of ignoring the fact that the ground state is a superconductor. Below we start from a superconductor and show that the scattering rate is free of singularities at $\omega = O(\Delta)$. To set the benchmark for the calculations in a superconductor, we make two observations. First, the full backscattering amplitude contains the sum of the contributions from different pairing channels, because the backscattering process involves vanishingly small total and transfer momentum. To the leading order in ϵ, partial amplitudes in channels with different angular momenta are equal, and their sum yields the two last terms in the right-hand side of Eq. (5). At $\ell = 1$, this contribution tends to a constant $2\mathrm{Li}_2(1) = \pi^2/3$, although its derivative is singular at $\ell = 1$. Beyond the leading order, the s-wave

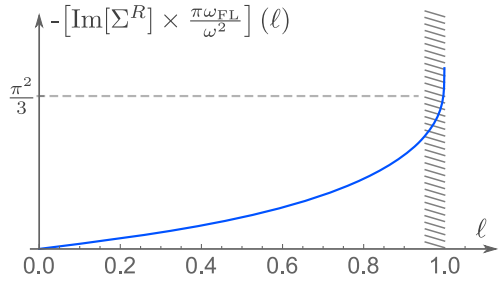

FIG. 1. Scattering rate divided by ω^2 as given by Eq. (5), for $\epsilon = 0.05$. Inside the dashed region, the normal state results are no longer valid.

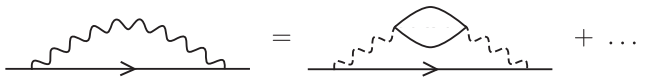

FIG. 2. Fermionic self-energy from excitation of a nematic fluctuation. Dashed wavy lines indicate a bare (static) nematic propagator.

component of the scattering amplitude is the largest, and the s-wave pole in the backscattering amplitude gives rise to the first term in the right-hand side of Eq. (5). Second, Eq. (5) is obtained with the logarithmic accuracy and is valid up to $1-\ell = O(\lambda)$. At the edge of applicability, the s-wave pole contribution is of order ϵ^2/λ and is small compared to the combined contribution from all pairing channels, i.e., $\mathrm{Im}[\Sigma^R(\omega)] \simeq (\Delta^2/\omega_{\mathrm{FL}})$. Below we compare this expression with the result that we obtain starting from a superconducting ground state.

Nematic propagator in the superconducting state.—The scattering rate in a superconductor is determined by the same process as in the normal state—a decay into a nematic fluctuation and another fermion (Fig. 2) [30]. However, in a superconductor both the fermionic propagator $G(q)$ and the polarization $\Pi(q)$ for nematic fluctuations get modified by the pairing gap Δ. The modification of $G(q)$ is well known [32], but the modification of $\Pi(q)$ is model specific. In our case, a straightforward analysis yields

$$\Pi(q) = 2\int_p f_{\boldsymbol{q}}(\boldsymbol{p})^2 \times [G(p+q/2)G(p-q/2) - F(p+q/2)F(p-q/2)], \tag{6}$$

where $q=(\Omega,\boldsymbol{q})$ and G and F are normal and anomalous Green's functions. The sign of the FF term is the same as for the spin polarization operator at $\boldsymbol{q}=(\pi,\pi)$ in a d-wave superconductor [33]. Like there, the dynamical bosonic propagator $D^R(\boldsymbol{q}=0)$ then contains a resonance at $\Omega<2\Delta$, when $g\mathrm{Re}[\Pi(\Omega,0)]+M^2=0$ [12]. One can view the nematic resonance as a particle-hole bound state within the two-particle gap; it originates from a residual interaction between Bogoliubov quasiparticles in a superconductor, which is attractive, like the original 4-fermion pairing interaction (1). We note that such resonance does not appear in the density-density correlator (a dressed particle-hole bubble with s-wave form factors), as there $\Pi(\Omega,\boldsymbol{q}=0)$ has to vanish to respect charge conservation [34,35]. On a technical level, this holds because the $GG-FF$ contribution cancels out by the contribution containing GF combinations and vertex corrections [35]. For the nematic correlator that we consider, there is no cancellation and the physics can be captured by keeping only $GG-FF$ terms (see the Supplemental Material [36] for more discussion on this).

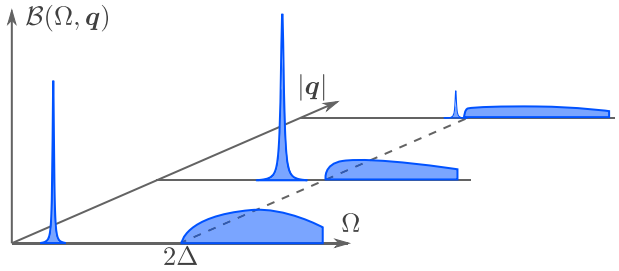

FIG. 3. Sketch of the nematic fluctuation spectrum $\mathcal{B}(\Omega,\boldsymbol{q}) = -\mathrm{Im}[D^R(\Omega,\boldsymbol{q})]$.

We present the full analysis of $\Pi^R(q)$ in our case in the Supplemental Material [36] and here quote the results. We have, at $\Omega \ll \Delta$,

$$\Pi^R(q) = \begin{cases} -\frac{\rho}{6}\times\frac{\Omega^2}{\Delta^2} - i0^+\mathrm{sign}(\Omega), & v_F|\boldsymbol{q}| \ll \Delta \\ -\frac{\pi\rho}{4}\times\frac{\Omega^2}{\Delta v_F|\boldsymbol{q}|} - i0^+\mathrm{sign}(\Omega), & v_F|\boldsymbol{q}| \gg \Delta \end{cases}. \tag{7}$$

The existence of the two regimes is specific to our case of small-$\boldsymbol{q}$ fluctuations and originates from the $1/|\boldsymbol{q}|$ dependence of the Landau damping in the normal state. Substituting $\Pi^R(q)$ into $D^R(q)$, we find that $\mathcal{B}=-\mathrm{Im}[D^R]$ consists of a resonance (a pole) and a continuum, $\mathcal{B}(q)=\mathcal{B}_{\mathrm{res}}(q)+\mathcal{B}_{\mathrm{cont}}(q)$; see Fig. 3. The resonance describes a 2D plasmonlike propagating quasiparticle whose position and the spectral weight strongly depend on the ratio $v_F|\boldsymbol{q}|/\Delta$. We find

$$\mathcal{B}_{\mathrm{res}}(q) = a_{\boldsymbol{q}}\times\delta[\Omega-\Omega_{\mathrm{res}}(\boldsymbol{q})],$$
$$\Omega_{\mathrm{res}}(\boldsymbol{q}) \sim \begin{cases} \Delta\times\sqrt{\epsilon/\lambda} & v_F|\boldsymbol{q}| \ll \Delta \\ \sqrt{\Delta v_F|\boldsymbol{q}|}\times\sqrt{\epsilon/\lambda} & v_F|\boldsymbol{q}| \gg \Delta \end{cases}, \tag{8}$$

and $a_{\boldsymbol{q}}$ varies between $a_{\boldsymbol{q}}\sim\Delta$ at $v_F|\boldsymbol{q}|\ll\Delta$ and $a_{\boldsymbol{q}}\sim\sqrt{\Delta v_F|\boldsymbol{q}|}$ at $v_F|\boldsymbol{q}|\gg\Delta$. At small ϵ and $v_F|\boldsymbol{q}|\sim\Delta$, $\Omega_{\mathrm{res}}(\boldsymbol{q})$ is much smaller than Δ.

The continuum $\mathcal{B}_{\mathrm{cont}}(q)$ sets in at $\Omega=2\Delta$ (see Ref. [36] for details). The full $\mathcal{B}(\Omega,\boldsymbol{q})$ is sketched in Fig. 3. For $v_F|\boldsymbol{q}|\sim\Delta$, the resonance is well separated from the continuum, but once $v_F|\boldsymbol{q}|$ exceeds $\Delta(\lambda/\epsilon)$, the resonance approaches the continuum, and its weight becomes exponentially small. Likewise, a small-weight resonance close to $\Omega=2\Delta$ is obtained for very weak coupling when ϵ/λ becomes too large [37].

Fermionic scattering rate at $\omega\sim\Delta$.—With $\mathcal{B}(\Omega,\boldsymbol{q})$ at hand, one can straightforwardly compute the scattering rate using the spectral representation. We present the details in the Supplemental Material [36] and here list the results and present the plot of $\mathrm{Im}[\Sigma^R(\omega)]$, Fig. 4. We obtain

$$\mathrm{Im}[\Sigma^R(\omega)] \sim \begin{cases} \lambda\Delta\left(\frac{\epsilon}{\lambda}\right)^{1/4}, & 0 < \omega - \omega_{\mathrm{th}} \lesssim \frac{\Delta^3}{\omega_{\mathrm{FL}}{}^2}\left(\frac{\epsilon}{\lambda}\right)^{5/2} \quad \text{regime I} \\ \frac{\Delta^2}{\omega_{\mathrm{FL}}}\left(\frac{\epsilon^3}{\lambda}\right)^{1/2}\left(\frac{\Delta}{(\omega-\omega_{\mathrm{th}})}\right)^{1/2}, & \frac{\Delta^3}{\omega_{\mathrm{FL}}{}^2}\left(\frac{\epsilon}{\lambda}\right)^{5/2} \lesssim \omega - \omega_{\mathrm{th}} \lesssim \Delta\left(\frac{\epsilon}{\lambda}\right)^{1/2} \quad \text{regime II} \\ \frac{\lambda\Delta^2}{\omega_{\mathrm{FL}}}\left(\frac{(\omega-\omega_{\mathrm{th}})}{\Delta}\right)^{5/2}, & \Delta\left(\frac{\epsilon}{\lambda}\right)^{1/2} + \omega_{\mathrm{th}} \lesssim \omega \lesssim \Delta[3 + O(\lambda^2)] \quad \text{regime III} \\ \frac{\Delta^2}{\omega_{\mathrm{FL}}}\left(\frac{\omega-3\Delta}{\Delta}\right)^{1/2}, & \omega \gtrsim \Delta[3 + O(\lambda^2)] \quad \text{regime IV} \end{cases} . \tag{9}$$

The scattering rate described by Eq. (9) starts a threshold $\omega_{\mathrm{th}} = \Omega_{\mathrm{res}}(0) + \Delta$, where it jumps to a value that is larger than the benchmark normal state expression $\mathrm{Im}[\Sigma^R(\omega)] \sim \Delta^2/\omega_{\mathrm{FL}}$ by a large factor $\sim E_F/\Delta$. It remains almost constant in a narrow energy window (regime I) and decreases as $1/\sqrt{\omega - \omega_{\mathrm{th}}}$ (regime II), mirroring the familiar DOS enhancement in a superconductor. For increasing energies, the rate crosses through a minimum and grows again (regime III), which is due to the momentum dependence of the resonance position and weight. Finally, for $\omega > 3\Delta$ (regime IV), the rate acquires an additional contribution from scattering into the continuum, which gives rise to a kink in $\mathrm{Im}[\Sigma^R(\omega)]$. For $\omega = 3\Delta + O(\Delta)$, the rate becomes of the same order as the normal state result and gradually transforms into $\mathrm{Im}[\Sigma^R(\omega)]$ from Eq. (5).

In Fig. 5 we plot the fermionic spectral function $\mathcal{A}(\omega) = (1/\pi)\mathrm{Im}[G^R(\omega)]$ at $\omega > \Delta$. At $\lambda \ll 1$, $\mathcal{A}(\omega) \propto \mathrm{Im}[\Sigma^R(\omega)]$. In this situation the most prominent feature, besides a sharp quasiparticle peak at $\omega = \Delta$, is a narrow peak at ω_{th}, followed by a broad minimum and a cusp at 3Δ. At larger frequencies where the normal state results are valid, a "hump" develops. This behavior can be termed as "peak-peak-dip-hump." At $\lambda \geq 1$, where $\mathrm{Im}[\Sigma^R(\omega)] > \Delta$ at $\omega \geq \omega_{\mathrm{th}}$, we expect that the peak at ω_{th} is suppressed, as in this situation $A(\omega) \propto 1/\mathrm{Im}[\Sigma^R(\omega)]$. Then the spectral function displays a peak-dip-hump behavior, similar to the one in the cuprates [10]. Since $\lambda \propto 1/M$, we expect a crossover from the peak-peak-dip-hump line shape to the peak-dip-hump one as the system comes closer to a nematic QCP.

We now analyze how the results are modified for lattice systems. For $d_{x^2-y^2}$ symmetry, the nematic form factor is $f(\boldsymbol{k}) = \cos k_x - \cos k_y$; it reduces to $f(\boldsymbol{k}) \propto \cos(2\theta_{\boldsymbol{k}\mathbf{n}_x})$ for small k_F. Such a form factor creates hot and cold regions on the Fermi surface. Our results for $\Sigma(\omega)$ are valid for the hot regions. The results hold with two modifications: (i) the jump of $\mathrm{Im}[\Sigma(\omega)]$ at ω_{th} is reduced by the relative width of the hot region and (ii) there exists a small but finite background $\mathrm{Im}[\Sigma(\omega)]$ from scattering into cold regions, where the gap is small [38].

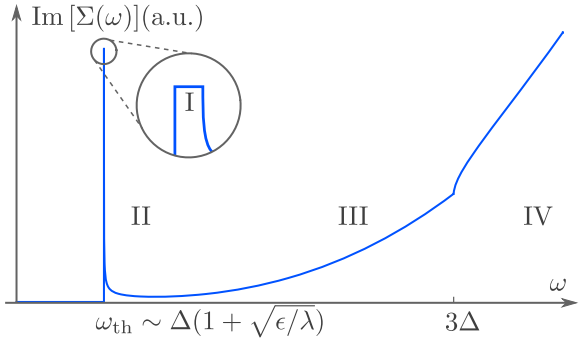

FIG. 4. Fermionic scattering rate, with scaling regimes as in Eq. (9). Used parameters: $\lambda = 0.4$, $\epsilon = 0.06$.

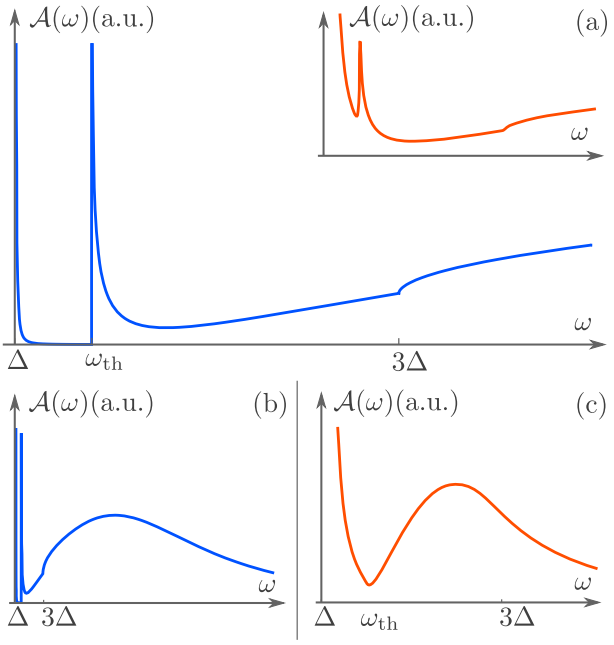

FIG. 5. Fermionic spectral function $\mathcal{A}(\omega)$ with the same parameters as in Fig. 4. (a) $\mathcal{A}(\omega)$ for $\omega \lesssim 3\Delta$, showing the peak-peak-dip structure. In the inset, $\mathcal{A}$ is broadened with a phenomenological quasiparticle width $\Gamma = 0.2\lambda\exp(-1/\lambda)$, due to additional processes such as impurity scattering. (b) $\mathcal{A}(\omega)$ at larger frequencies, showing the hump. (c) *Sketch* of $\mathcal{A}$ for $\omega \lesssim 3\Delta$, $\Gamma > 0$ and strong coupling $\lambda > 1$, showing conventional peak-dip-hump features.

Conclusion.—We analyzed the propagator of soft nematic fluctuations and fermionic scattering rate $\mathrm{Im}[\Sigma^R(\omega)]$ of fermions in an s-wave SC state near a nematic QCP. We argued that $\mathrm{Im}[\Sigma^R(\omega)]$ is qualitatively different from that in an ordinary s-wave SC because near a QCP, the pairing interaction in the s-wave channel is only slightly larger than in pairing channels with other angular momenta. We showed that the spectrum of nematic fluctuations in a SC consists of a gapped continuum and a strongly dispersing resonance mode. We found three different regimes of the scattering rate, due to the interaction with a resonance: a jump at the threshold, a decrease towards a shallow minimum, and a slow subsequent increase. A fourth regime is realized at $\omega \geq 3\Delta$, when the scattering rate predominantly comes from the interaction with the continuum. At higher frequencies, $\mathrm{Im}[\Sigma^R(\omega)]$ gradually transforms into the normal state expression. This leads to a peak-peak-dip-hump structure of the fermionic spectral function. This structure transforms into the more familiar peak-dip-hump line shape as the system comes closer to a nematic QCP and the coupling constant λ increases.

Superconductivity at the onset of a nematic order at $T = 0$ develops in several systems studied in recent years, most notably in $FeSe_{1-x}S_x$ around $x = 0.2$. We call for ARPES measurements of the fermionic spectral function to verify our results.

The work by A. V. C. was supported by the Office of Basic Energy Sciences, U.S. Department of Energy, under Award No. DE-SC0014402. A. K. was supported by NSF Grant No. DMR-2037654.

*dpimenov@umn.edu

[1] H. F. Fong, B. Keimer, D. Reznik, D. L. Milius, and I. A. Aksay, Phys. Rev. B **54**, 6708 (1996).
[2] P. Dai, H. A. Mook, S. M. Hayden, G. Aeppli, T. G. Perring, R. D. Hunt, and F. Doğan, Science **284**, 1344 (1999).
[3] P. Bourges, Y. Sidis, H. F. Fong, L. P. Regnault, J. Bossy, A. Ivanov, and B. Keimer, Science **288**, 1234 (2000).
[4] J. C. Campuzano, H. Ding, M. R. Norman, H. M. Fretwell, M. Randeria, A. Kaminski, J. Mesot, T. Takeuchi, T. Sato, T. Yokoya, T. Takahashi, T. Mochiku, K. Kadowaki, P. Guptasarma, D. G. Hinks, Z. Konstantinovic, Z. Z. Li, and H. Raffy, Phys. Rev. Lett. **83**, 3709 (1999).
[5] Z.-X. Shen, P. J. White, D. L. Feng, C. Kim, G. D. Gu, H. Ikeda, R. Yoshizaki, and N. Koshizuka, Science **280**, 259 (1998).
[6] J. F. Zasadzinski, L. Ozyuzer, N. Miyakawa, K. E. Gray, D. G. Hinks, and C. Kendziora, Phys. Rev. Lett. **87**, 067005 (2001).
[7] T. Valla, A. V. Fedorov, P. D. Johnson, B. O. Wells, S. L. Hulbert, Q. Li, G. D. Gu, and N. Koshizuka, Science **285**, 2110 (1999).
[8] A. Kaminski, J. Mesot, H. Fretwell, J. C. Campuzano, M. R. Norman, M. Randeria, H. Ding, T. Sato, T. Takahashi, T. Mochiku, K. Kadowaki, and H. Hoechst, Phys. Rev. Lett. **84**, 1788 (2000).
[9] J. Fink, A. Koitzsch, J. Geck, V. Zabolotnyy, M. Knupfer, B. Büchner, A. Chubukov, and H. Berger, Phys. Rev. B **74**, 165102 (2006).
[10] M. Eschrig, Adv. Phys. **55**, 47 (2006).
[11] A. Abanov, A. V. Chubukov, and J. Schmalian, J. Electron Spectrosc. Relat. Phenom. **117–118**, 129 (2001).
[12] Y. Gallais, I. Paul, L. Chauvière, and J. Schmalian, Phys. Rev. Lett. **116**, 017001 (2016).
[13] V. K. Thorsmølle, M. Khodas, Z. P. Yin, C. Zhang, S. V. Carr, P. Dai, and G. Blumberg, Phys. Rev. B **93**, 054515 (2016).
[14] A. Hinojosa, J. Cai, and A. V. Chubukov, Phys. Rev. B **93**, 075106 (2016).
[15] S.-F. Wu, P. Richard, H. Ding, H.-H. Wen, G. Tan, M. Wang, C. Zhang, P. Dai, and G. Blumberg, Phys. Rev. B **95**, 085125 (2017).
[16] T. Adachi, M. Nakajima, Y. Gallais, S. Miyasaka, and S. Tajima, Phys. Rev. B **101**, 085102 (2020).
[17] S. Lederer, Y. Schattner, E. Berg, and S. A. Kivelson, Phys. Rev. Lett. **114**, 097001 (2015).
[18] A. Klein, Y.-M. Wu, and A. V. Chubukov, npj Quantum Mater. **4**, 55 (2019).
[19] A. E. Böhmer and A. Kreisel, J. Phys. Condens. Matter **30**, 023001 (2018).
[20] W. Metzner, D. Rohe, and S. Andergassen, Phys. Rev. Lett. **91**, 066402 (2003).
[21] A. Abanov, A. V. Chubukov, and J. Schmalian, Adv. Phys. **52**, 119 (2003).
[22] S. Graser, T. A. Maier, P. J. Hirschfeld, and D. J. Scalapino, New J. Phys. **11**, 025016 (2009).
[23] M. A. Metlitski and S. Sachdev, Phys. Rev. B **82**, 075127 (2010).
[24] S.-S. Lee, Phys. Rev. B **80**, 165102 (2009).
[25] D. L. Maslov and A. V. Chubukov, Phys. Rev. B **81**, 045110 (2010).
[26] We note that the finite M cuts off the logarithmic flow of λ, while right at the QCP this flow is cut off by the onset of pairing.
[27] C. J. Halboth and W. Metzner, Phys. Rev. B **57**, 8873 (1998).
[28] A. V. Chubukov, D. L. Maslov, S. Gangadharaiah, and L. I. Glazman, Phys. Rev. B **71**, 205112 (2005).
[29] D. Pimenov, A. Kamenev, and A. V. Chubukov, Phys. Rev. B **103**, 214519 (2021).
[30] For sufficiently long-range interactions (small M), the rate may be influenced by additional collective low-energy excitations, see Refs. [18,31].
[31] K. Yang and S. L. Sondhi, Phys. Rev. B **62**, 11778 (2000).
[32] A. A. Abrikosov, L. P. Gorkov, and I. E. Dzyaloshinski, *Methods of Quantum Field Theory in Statistical Physics* (Courier Corporation, New York, 2012).
[33] In the latter case, there are two additional minus signs that compensate each other: one due to the presence of spin σ matrices in the vertices, and another due to the sign change of a d-wave gap between $\boldsymbol{k}$ and $\boldsymbol{k} + \boldsymbol{q}$.

[34] T. Cea and L. Benfatto, Phys. Rev. B **94**, 064512 (2016).
[35] S. Maiti, A. V. Chubukov, and P. J. Hirschfeld, Phys. Rev. B **96**, 014503 (2017).
[36] See Supplemental Material at http://link.aps.org/supplemental/10.1103/PhysRevLett.128.017001 for further technical details.
[37] For $\epsilon/\lambda > 1$, the resonance condition can still be fulfilled below the continuum threshold due to divergence of $\Pi^R(\Omega \nearrow 2\Delta)$, see the Supplemental Material [36].
[38] A. Klein and A. Chubukov, Phys. Rev. B **98**, 220501(R) (2018).